Neck Soft Tissue Injury Mechanism in side Blast Events

Bastien, H.[1], Bouamoul, A.[2], Rancourt, D.[1]
[1]Groupe de recherche PERSEUS, Université de Sherbrooke, Sherbrooke, QC, Canada, J1K2R1
[2]DRDC Valcartier, 2459, boul. Pie-XI nord, Québec (Québec), Canada, G3J 1X5

Original Article

15/12/2009

For correspondence:
Denis Rancourt, PhD, MScA, ing.
Groupe de Recherche Perseus
Université de Sherbrooke
2500, boul. de l'Université Sherbrooke (Québec)
CANADA J1K 2R1
Tel: 819-821-8000 p: 61346
Fax: 819-821-7163
Email: denis.rancourt@usherbrooke,ca

Keywords: whiplash, side blast, neck model, soft connective tissues.

2677 words

Abstract

Injuries caused by high impact events such as side blasts and mines on light armoured vehicles (LAV) are an important concern for army forces. Side blast event is blasts (e.g. roadside bombs, improvised explosive devices) that strike the sides of vehicles. This paper presents an anatomical finite element model of the human neck used to study armour vehicle occupants. The model was used to identify which anatomical structures may suffer damage and in what order following a side blast event. A velocity profile of the torso was simulated based upon results obtained from DRDC Valcartier with a vertical drop tower. Head and vertebrae were modelled as rigid bodies and their dimensions were adjusted to accurately locate muscles and ligament attachments. Nuchal and anterior longitudinal ligaments were included because of their stabilizing role in body joints during large motions. Seven muscles groups were modelled: the trapezius, the levator scapulae, the longissimus, the longus, the scalenus, the splenius capitis and the sternocleidomastoid. Muscle models included fasciae to investigate whether fascia would play a significant role in restraining neck motion. Since fascia mechanical properties are not well documented, a sensitivity analysis was performed with the model, varying fascia stiffness to evaluate their impact on the model results. Simulation results showed that the anterior longitudinal ligament strain reaches a maximum of 20% in the C7-T1 portion and up to 100 % at the C0-C1 level. Simulation results showed also that soft connective tissues experienced important strain rates, as high as 20.000 mm/mm/s in the higher portion (C0-C1) of the anterior longitudinal ligament.

Introduction

Injuries to occupants of light armoured vehicles (LAV) caused by high impact events such as side blast events and improvised explosive devices are an important concern for army forces. There is a need to develop protective devices to limit injuries during such events. Because of ethical issues associated with studying such injuries using biological surrogates, models must be developed to predict the performance of protective devices. The design of such devices is challenging because of the high accelerations encountered, in the range of 80 g for a few milliseconds. Currently, the use of experimental or numerical models of mannequins is a common approach to the problem (Williams and Fillion-Gourdeau (2002)). Mannequins (e.g. the Hybrid III) show some benefits because they can provide experimental data such as forces or accelerations that can be used to predict injuries. Although mannequin kinematics/kinetics may be close to those of a real human body, results from numerical models of mannequins can be misleading because they may not adequately represent the mechanisms underlying the injuries. For instance, current injury evaluation uses global scale indices (i.e. HIC (Tabiei and Nilakantan (2007))) as injury criteria, suggesting possible event outcomes (i.e. probability of death) based on statistical studies. Specific effects on anatomical structures (e.g. muscles and ligaments) and the evolution of the injury during the event may be more meaningful but they are usually not addressed. Only by knowing the detailed response of the various structures of the body and by understanding how those reactions lead to a fatal injury can appropriate mitigation strategies be designed.

The aim of this study was to develop an anatomical numerical model of a human body in side blasts events, with sufficient detail to identify which anatomical structures may sustain injuries and in what order. This information is essential to focus the design of protective devices on the exact nature of body injuries. Because of the complexity involved in developing such a model, we have focused our attention to the neck region which is susceptible to injuries in side blast incidents. The model developed was used to determine the resulting kinematics of the neck and its internal anatomical structures during a side-blast event. Results provided new insights on a non-intuitive injury mechanism suggesting that the anterior ligament is first injured following a hyperextension rebound of the neck, a few milliseconds following the blast event. A sensitivity analysis of the anatomical structures (muscles & ligaments)

involved in the model was performed and showed that muscles have little influence on soft tissue strains while ligaments are the most loaded and strained structures.

Methodology

A finite element (FE) model of a human body seated laterally in a LAV was developed for LS-Dyna™. A vertical drop tower testing facility developed by DRDC Valcartier was used to determine a velocity profile of the torso during a typical side blast event. The drop tower was designed specifically to reproduce the types of loading seen in experimental assessments of armour vehicle occupant reactions to buried charges and side attack blast. A detailed model of the trunk and neck was developed to identify which anatomical structures may sustain damage during a blast event and in what order. Building a new model from scratch was required because neither actual mannequins nor their associated FE models are detailed enough for that purpose. They do provide rigid body kinematics and joint forces or moments but they provide no information on the loading of the detailed anatomical structures. Such information is important because protective devices should primarily target the critical structures which are injured first. Given the complexity of the human body, the model was limited to the neck, as it is one of the human body regions susceptible to injuries in these types of events. Neck models have been developed previously (Bourdet and Willinger (2008), Linder (2000), Küçük (2007)), but these models showed important limitations concerning damage sustained by soft tissues. Soft tissues (muscles and ligaments) are sometimes modelled with 1D-elements (Van Lopik and Acar (2004), Wittek et *al.* (2001)) to include their influence on head motion. However, since soft tissues are not explicitly represented, stress and strain evaluation is limited. A study of soft tissues injury is not feasible with this approach.

Given the potential of high strain rates that might be encountered in side blast events, a more detailed model of the neck which captured detailed anatomical structures had to be developed. These structures (tendons, ligaments, muscles, fascia) are made of connective tissues which exhibit a hyperelastic and viscoelastic behaviour (Limbert and Middleton (2006), Ciarletta et *al.* (2008)) that may lead to unexpected high stresses in the structures during a blast event. This is due, for instance, to changes in their dynamic stiffness with strain rate. It has been reported that

increasing strain-rate causes an increase in soft tissue stiffness (Crisco et *al.* (2002), Haut and Haut (1997), Panjabi et *al.* (1998), Koh et *al.* (2004), Ng et *al.* (2004)).

Head and vertebrae were modelled as rigid bodies and their dimensions were adjusted to accurately locate muscles and ligaments attachments according to McMinn (1993) (cf. Figure 1 and Table 1). Vertebrae densities were adjusted individually to simulate individual vertebrae masses (Stemper et *al.* (2006)). Inter-Vertebral (IV) discs were modelled with 3D elements that can predict the shear stress experienced by each disc. The IV discs' mechanical properties were adjusted to approach rigidities reported by Küçük (2007) (cf. Table 2). A torsion spring element was located at joint C0-C1 while joint C1-C2 had to be stiffened slightly to avoid numerical instabilities.

Ligaments were also included in the numerical model because of their stabilizing role in the joint articulations during large joint motions. Both the nuchal and the anterior longitudinal ligaments were modelled using shell elements (assuming a uniform thickness of 2 mm) to study stress and strain distribution. Ligament material properties were adjusted using data from Stemper et *al.* (2006), with a Young modulus of 19 MPa.

Seven important muscles groups were modelled. They are the trapezius, the levator scapulae, the longissimus, the longus, the scalenus, the splenius capitis and the sternocleidomastoid. These seven groups were considered because they are known to play a significant role in controlling head motion during impacts (Conley et *al.* (1997)). Each muscle core was modelled using 3D elements and a linear isotropic constitutive model with a Young modulus of 11 MPa, and the bulk material was surrounded by an envelope (a connective tissue fascia) modelled with shell elements with different mechanical properties. Since fascia mechanical properties are not well documented, a sensitivity analysis was performed in the numerical simulations varying fascia stiffness to evaluate its impact on the results. Kureshi et *al.* (2008) has measured transversalis fascia Young modulus between 0.4 MPa and 10 MPa. Zeng et *al.* (2003)'s study on nasal fascia showed a modulus around 6 MPa. Since these two studies were performed at very low strain rate and an increase of strain rate is known to cause a stiffening of soft connective tissues (Crisco et *al.* (2002), Haut and Haut (1997), Panjabi et *al.* (1998), Koh et *al.* (2004), Ng et *al.* (2004)), a nominal Young modulus of 22 MPa was used throughout the model. This simplified fascia-bulk material model of a muscle, inspired from the

work of Hukins *et al.* (1990), is unusual but it provides, from our point of view, a much better muscle approximation since fascia is more susceptible to high strain rate lesions because of its higher stiffness. The cross-sectional area for each muscle was based on MRI measurements on 20 active students (Conley et *al.* (1997)) and muscular density was set to 1.112 g/cm^3 (Ward and Lieber (2005)). Table 3 summarizes the origin and insertion and number of elements used in each muscle model.

Although the overall model was three-dimensional in nature, the input to the model was a planar motion of muscle and ligament attachments at the torso level. As mentioned above, that proscribed motion was based on results obtained with a vertical drop tower testing facility developed at DRDC Valcartier (Figure 2). All material properties were assumed to be linear as a first approximation. Computer simulations were performed with LS-DYNA 971 software on MAMMOUTH-SERIE II (A super-computer of the Réseau Québécois de Calcul de Haute Performance with a peak compute performance of 27 596 GFlops).

Results

Simulation results showed that the anterior longitudinal ligament strain reaches a maximum of 20% in the C7-T1 portion and up to 100% at the C0-C1 level, causing an excessive hourglass of the elements that led to termination (Figure 3). There are two moments where the anterior longitudinal ligament reaches a peak deformation. Firstly, it occurs when the head reaches its maximal backward position (at ~30ms, Figure 3). At that moment, the lower neck experiences tension and the lower portion of the anterior longitudinal ligament (between C7-T1) is maximally deformed (18%) and the upper portion (C0-C1) does not experience any tension (upper neck flexion). Secondly, after reaching that position, the head bounces forward (Figure 3) and the upper neck experiences a hyperflexion until the strain in the C0-C1 anterior longitudinal ligament portion becomes excessive, leading to simulation termination. The nuchal ligament strain reaches 35% while the head bounces forward and its recoil is the cause of the anterior longitudinal ligament high deformation in the upper (C0-C1) portion (Figure 4). The nuchal ligament reaches a maximal deformation at the same time (~30ms) as the anterior longitudinal ligament lower (C7-T1) portion. The

nuchal ligament experiences its maximal strain locally near C1. A sensitivity analysis of the ligaments and muscle fascia mechanical properties showed that only ligaments affected head motion significantly (Figure 5). Hence, mechanical properties of ligaments are critical in determining the gravity of neck injuries. The trapezius and sternocleidomastoid fasciae experienced a maximal deformation of 14% (Figure 6).

Simulation results showed that soft connective tissues experienced important strain rates. The higher portion (C0-C1) of the anterior longitudinal ligament experienced a strain-rate of 20 000%/s over the entire inter-vertebral region. The nuchal ligament reached 4000 %/s in the same region (C0-C1) over a relatively wide area. Fasciae also showed important strain rates but more locally and over shorter time intervals. While strain rates of levator scapulae and splenius capitis fasciae remained negligible, other fasciae (trapezius, longissimus, scalenus, sternocleidomastoid and longus) reached as high as 10 000 to 20 000 %/s.

Discussion

The underlying assumption of this study was that the design of effective protective devices against side blasts requires more detailed information than rigid body motion of grossly interconnected segments and HIC magnitude. As a matter of fact, because the human body is exposed to very high acceleration and velocity levels during side blasts, injuries are not solely related to body segment impacts with the surroundings (e.g. Wang et *al.* (2005)) but, probably and more importantly, to excessive segmental and intersegmental motion (both range and strain rate) which may cause soft tissue lesions. Currently available dummies for experimental testing (and their numerical models) do not include soft tissues structures and therefore can not provide critical information in this regard.

The goal of the model developed in this study was to gain more insights on the mechanism of neck injury following side blast event; that is, blasts that strike the sides of vehicles to the rear of its occupants which are typically seated in a transverse direction of the vehicle. Given the complexity of modelling the entire anatomical structure of the body, the effort reported on here was limited to the neck region. There is no surprise that the anterior longitudinal ligament was found to be the highly solicited part in head hyperextension. The new insight that emerged from the simulations

performed here is that this hyperextension follows a rebound from a hyperflexion of the neck, assuming that the nuchal ligament can sustain the load. Otherwise, it is the nuchal ligament that fails first. In any case, failure of the nuchal ligament or the anterior longitudinal ligament in the C0-C1 region may lead to C0-C1 dislocation. At the same time, the trapezius and sternocleidomastoid muscles (and their related fasciae) are injured however they are not the primary cause of serious injuries. The injury mechanism proposed here suggests that both head hyperextension and hyperflexion should be limited by protective devices to limit neck injuries.

Deformations of the inferior portion of the anterior longitudinal ligament are similar to those reported by Ivancic et *al.* (2004) who used a whole cervical spine mechanical model for studying whiplash. From C2 to C7, their strain levels were between 15% and 30 % at 8g while the one simulated in this study were between 12% and 30 %, but with a 80g peak for a very short duration. The anterior longitudinal ligament's high strain about C0-C1 has not been reported by Ivancic et *al.* (2004) but it may play an important role in the neck injury mechanism in side blast events. Use of a steel cable between C0 and C2 as a flexion limiter by Ivancic et *al.* (2004) has probably contributed to significantly limit the anterior longitudinal ligament strains about C0-C1 in their study. In contrast, our simulations showed considerable strain amplitude in that region, amplified by the elastic behaviour of the nuchal ligament, assuming no failure occurred for that ligament during the prior hyperflexion.

Simulation results were based on material properties that were assumed to be linear and strain rate independent. This is in conflict with the previous discussion on the fact that connective soft tissues are hyperelastic and viscoelastic. Soft tissue strain rates as high as 20 000 mm/mm/s (for the anterior longitudinal ligament) were found in the numerical simulations, indicating the need to include more sophisticated soft tissue models in further studies. In fact, if more realistic soft tissue strain rate dependent failure criteria were included in the simulations, the injury mechanism could potentially change. A literature survey on the impact of strain rate on soft tissue mechanical properties showed conflicting conclusions and one reason for such discrepancy is the difference in experimental protocols. Hopkinson bars (Kaiser (1998), Gray (1997)) are often used for evaluating soft tissue properties at high strain rates. While there are tensile Hopkinson bars, the vast majority of high rate testing of biological specimens study small samples in

compression without fixed boundary conditions to avoid liquid extrusion. In reality, soft tissues are mainly loaded and fail in tension in more or less confined fixed volumes.

The current model made a first attempt at including fascia in the muscle models to investigate whether the presence of the fascia would result in muscles playing a more significant role in restraining neck motion. The fascial muscle, although highly simplified, did not show additional muscle impact on neck motion which was shown to be associated with ligament restrictions. A refined model with more realistic fascia geometry and accurate mechanical properties dependent on strain rate could change the situation. Muscles are not only constructed from a strong outer fascia but are basically a honeycomb fascia structure filled with muscles cells (Kjaer (2004)).

Conclusions

This paper presented a finite element anatomical model of the neck to evaluate possible injury mechanisms that may occur during side blast events. Results showed that major strains occurred in the anterior longitudinal ligament during a neck hyperextension if a prior hyperextension-hyperflexion motion is made possible by the neck soft tissues i.e. if no failure occurred beforehand. Our study suggests that neck failure occurs at C0-C1 level and the design of protective devices should therefore focus on limiting both head extension and flexion to limit motion in that vertebral segment. Although the current model was based on linear material properties, results showed that soft tissues sustain very high strain rate, in the range of 20 000 mm/mm/s. Such levels indicate the need to include more realistic soft tissue strain rate dependent properties, including failure criteria. Fasciae were included in a new muscle model but despite this more accurate approach to modelling the muscles, simulations showed that protecting individuals by precontracting neck muscles is probably not an interesting approach to help limit neck injuries as the response is dominated by ligament response.

References

Bourdet, N., Willinger, R., 2008. Coupled head-neck-torso and seat model for car seat optimization under rear-end impact. Journal of Sound and Vibration 313, 891-907.

Ciarletta, P., Dario, P., Micera, S., 2008. Pseudo-hyperelastic model of tendon hysteresis from adaptative recruitment of collagen type I fibrils. Biomaterials 29, 764-770.

Conley, M. S., Stone, M. H., Nimmons, M., Dudley, G. A. 1997. Specificity of resistance training responses in neck muscle size and strength. European Journal of Applied Physiology 75, 443-448.

Crisco, J. J., Moore, D. C., McGovern, R. D., 2002. Strain-rate sensitivity of the rabbit MCL diminishes at traumatic loading rates. Journal of Biomechanics 35, 1379-1385.

Gray, G.T., 1997, High strain-Rate Testing of Materials: The Split Hopkinson Bar, Methods in Materials Research, John Wiley Press.

Haut, T. L., Haut, R. C., 1997. The state of tissue hydration determines the strain-rate-sensitive stiffness of human patellar tendon. Journal of Biomechanics 30, 79-81.

Hukins, D.W.L., Aspden, R.M., Hickey, D.S., 1990. Thoracolumbar fascia can increase the efficiency of the erector spinae muscles. Clinical Biomechanics 5:1, 30-34.

Ivancic, P. C., Pearson, A. M., Panjabi, M. M., Ito, S., 2004. Injury of the anterior longitudinal ligament during whiplash simulation. European Spine Journal 13, 61-68.

Kaiser, M.A., 1998, Advancements in the Split Hopkinson Bar Test. Thesis in Mechanical Engineering, Blacksburg, Virginia.

Kjaer, M., 2004. Role of extracellular matrix in adaptation of tendon and skeletal muscle to mechanical loading. Physiological Review 84, 649-698.

Koh, S.-W., Cavanaugh, J. M., Leach, J. P., Rouhana, S. W., 2004. Mechanical properties of the shoulder ligaments under quasi-static and dynamic loading. In ISB XXth Congress – ASB 29th Annual Meeting. Cleveland, Ohio.

Küçük, H., 2007. Biomechanical analysis of cervical spine sagittal stiffness characteristics. Computer in Biology and Medicine 37, 1283-1291.

Kureshi, A., Vaiude, P., Nazhat, S. N., Petrie, A., Brown, R.A., 2008. Matrix mechanical properties of transversalis fascia in inguinal herniation as a model for tissue expansion. Journal of Biomechanics 41, 3462-3468.

Limbert, G., Middleton, J., 2006. A constitutive model of the posterior cruciate ligament. Medical Engineering & Physics 28, 99-113.

Linder, A., 2000. A new mathematical neck model for a low-velocity rear-end impact dummy: evaluation of components influencing head kinematics. Accident Analysis and Prevention 32, 261-269.

McMinn, R. M. H., Hutchings, R. T., Pegington, J., Abrahams, P., 1993, Color Atlas of Human Anatomy, Third Edition., Mosby – Year Book, Inc.

Ng, B. H., Chou, S. M., Lim, B. H., Chong, A., 2004. Strain rate effect on the failure properties of tendons. Proc. Instn Mech. Engrs vol 218 Part H. Journal of Engineering in Medicine, 203-206.

Panjabi, M. M., Crisco, J. J., Lydon, C., Dvorak, J., 1998. The mechanical properties of human alar and transverse ligaments at slow and fast extension rates. Clinical Biomechanics 13:2, 112-120.

Stemper, B. D., Yoganandan, N., Pintar, F. A., Rao, R. D., 2006. Anterior longitudinal ligament injuries in whiplash may lead to cervical instability. Medical Engineering & Physics 28, 515-524.

Tabiei, A., Nilakantan, G., 2007. Reduction of acceleration induced injuries from mine blasts under infantry vehicles. In 6th European LS-DYNA Users' Conference. Gothenburg, Sweden. Livermore Software Technology Corporation (LSTC).

Wang, F., Lee, H. P., Lu, C., Cheng, Q. H., 2005. Evaluation of human head injury in tracked vehicle subjected to mine blast. In IUTAM Proceedings on Impact Biomechanics: From Fundamental Insights to Applications, 273-280. Springer. Netherlands

Van Lopik, D. W., Acar, M., 2004. A computational model of the human head and neck system for the analysis of whiplash motion. International Journal of Crashworthiness 9:5, 465-473.

Ward, S.R., Lieber, R.L., 2005. Density and hydration of fresh and fixed human skeletal muscle. Journal of Biomechanics 38:11, 2317-2320.

Williams, K., Fillion-Gourdeau, F., 2002. Numerical Simulation of light armoured vehicle occupant vulnerability to anti-vehicle mine blast. In 7th International LS-DYNA Users' Conference. Michigan, USA. Livermore Software Technology Corporation (LSTC) and Engineering Technology Associates (ETA).

Wittek, A., Kajzer, J., Haug, E., Ono, K., 2001. Finite element modelling of the muscle effects on kinematic responses of head-neck complex in frontal impact at high speed. JSME International Journal Series C 44:2, 379-388.

Zeng, Y.-J., Sun, X.-P., Yang, J., Wu, W.-H., Xu, X.-H., Yan, Y.-P., 2003. Mechanical properties of nasal fascia and periosteum. Clinical Biomechanics 18, 760-764.

LIST OF FIGURES

LIST OF TABLES

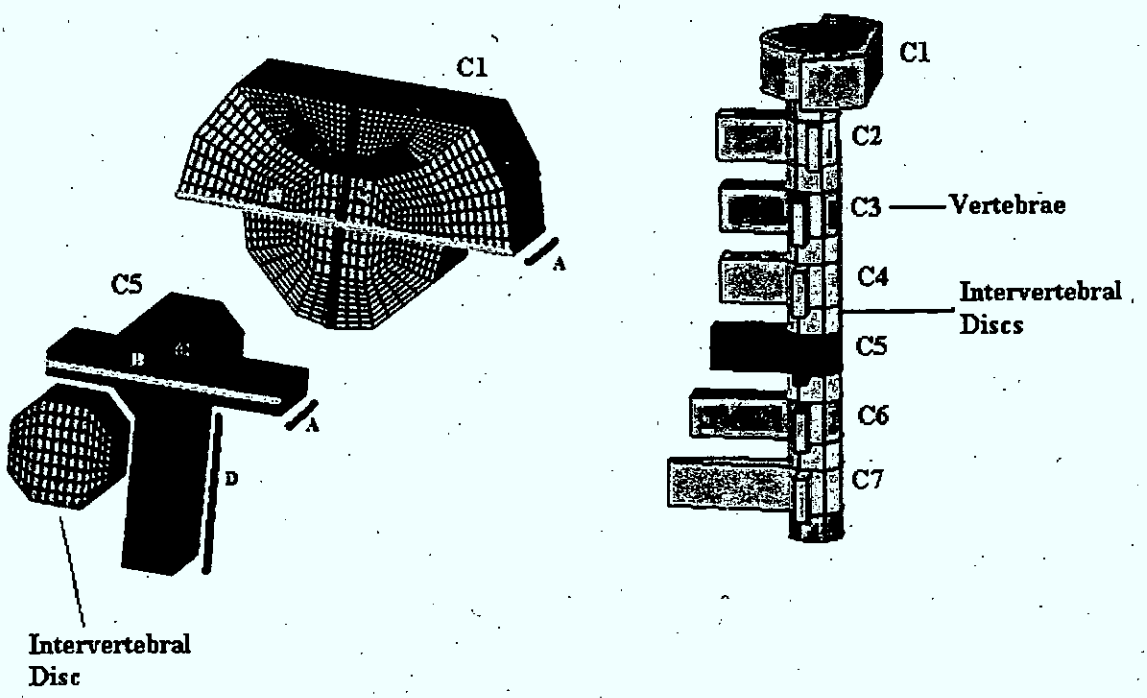
C1
A
C5
B
A
D
Intervertebral
Disc
C1
C2
C3
Vertebrae
C4
Intervertebral
Discs
C5
C6
C7

FIGURE 1

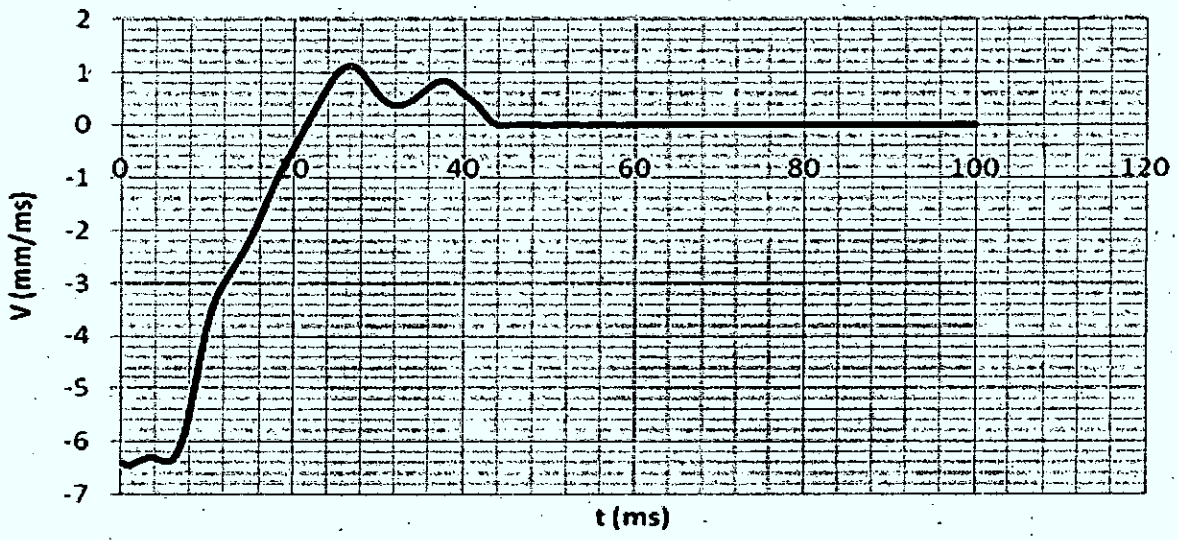

FIGURE 2

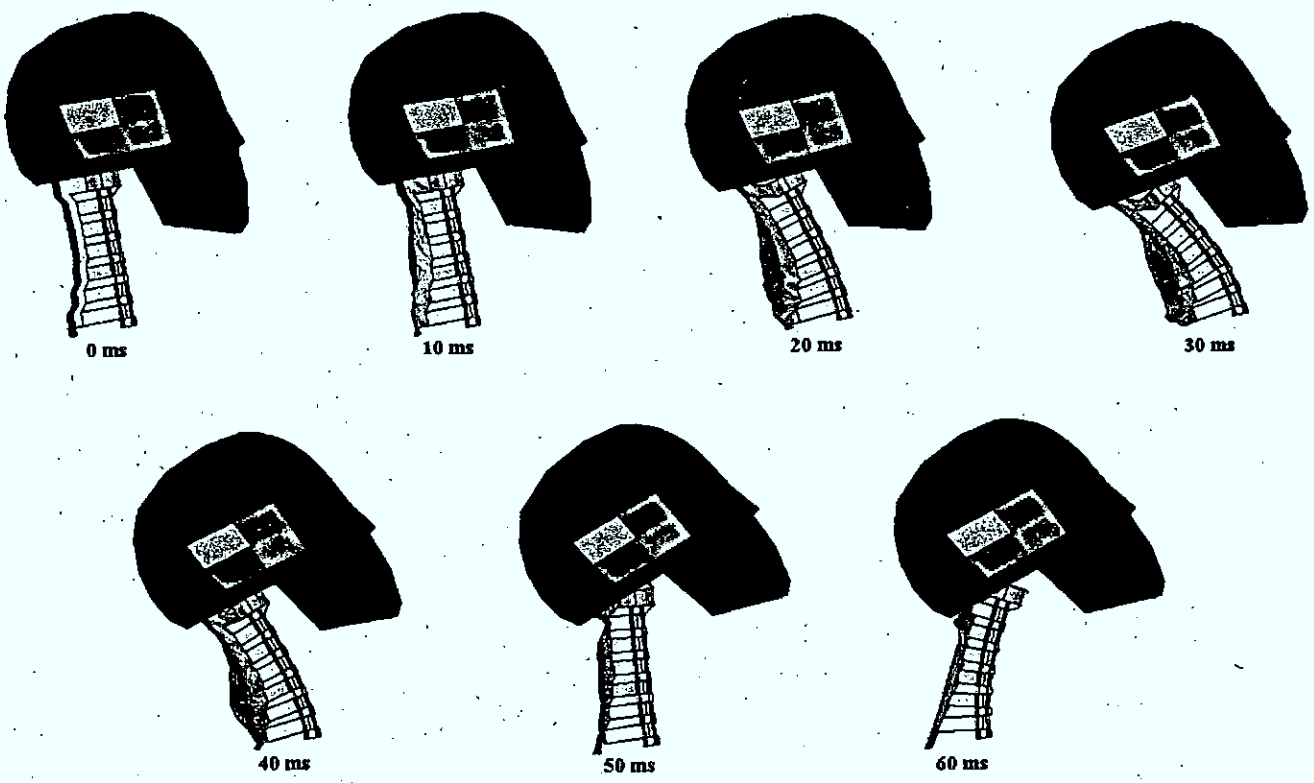

FIGURE 3

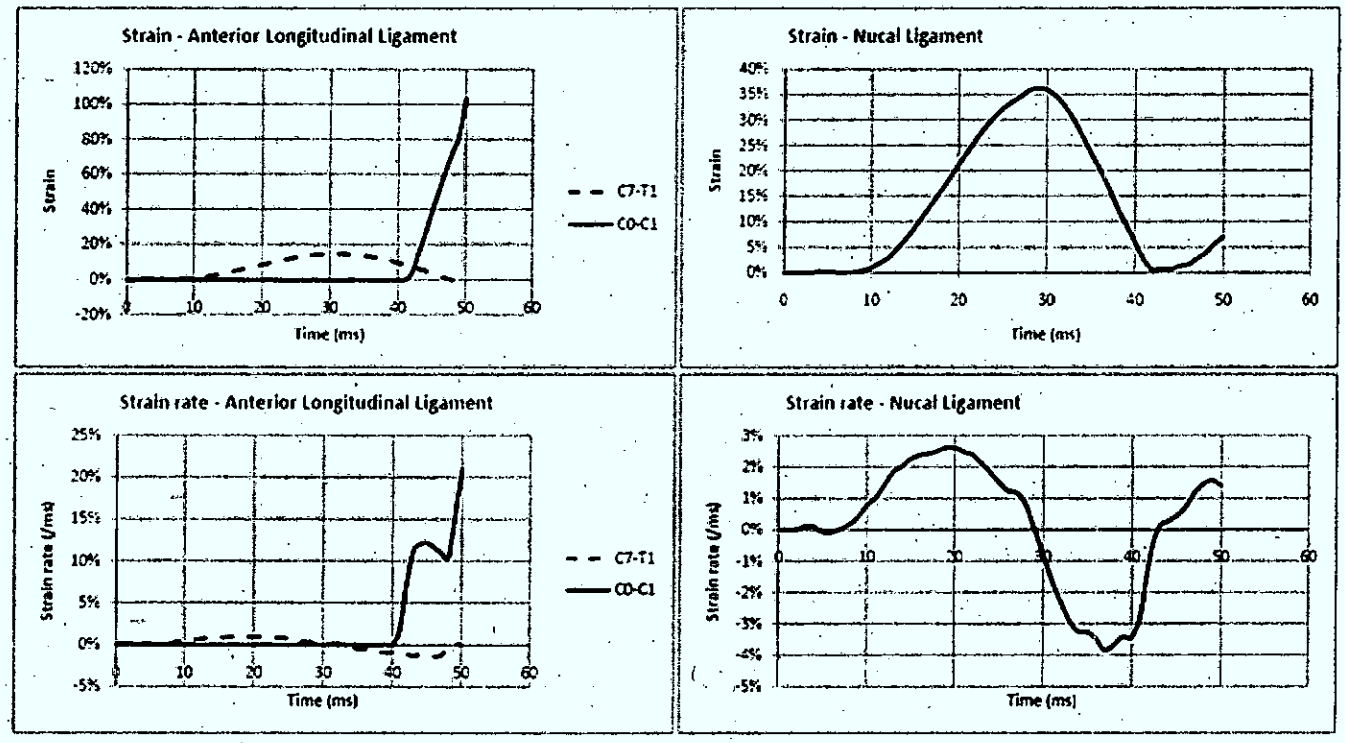
Strain - Anterior Longitudinal Ligament
Strain
Time (ms)
C7-T1
C0-C1
Strain - Nucal Ligament
Strain
Time (ms)
Strain rate - Anterior Longitudinal Ligament
Strain rate (/ms)
Time (ms)
C7-T1
C0-C1
Strain rate - Nucal Ligament
Strain rate (/ms)
Time (ms)

FIGURE 4

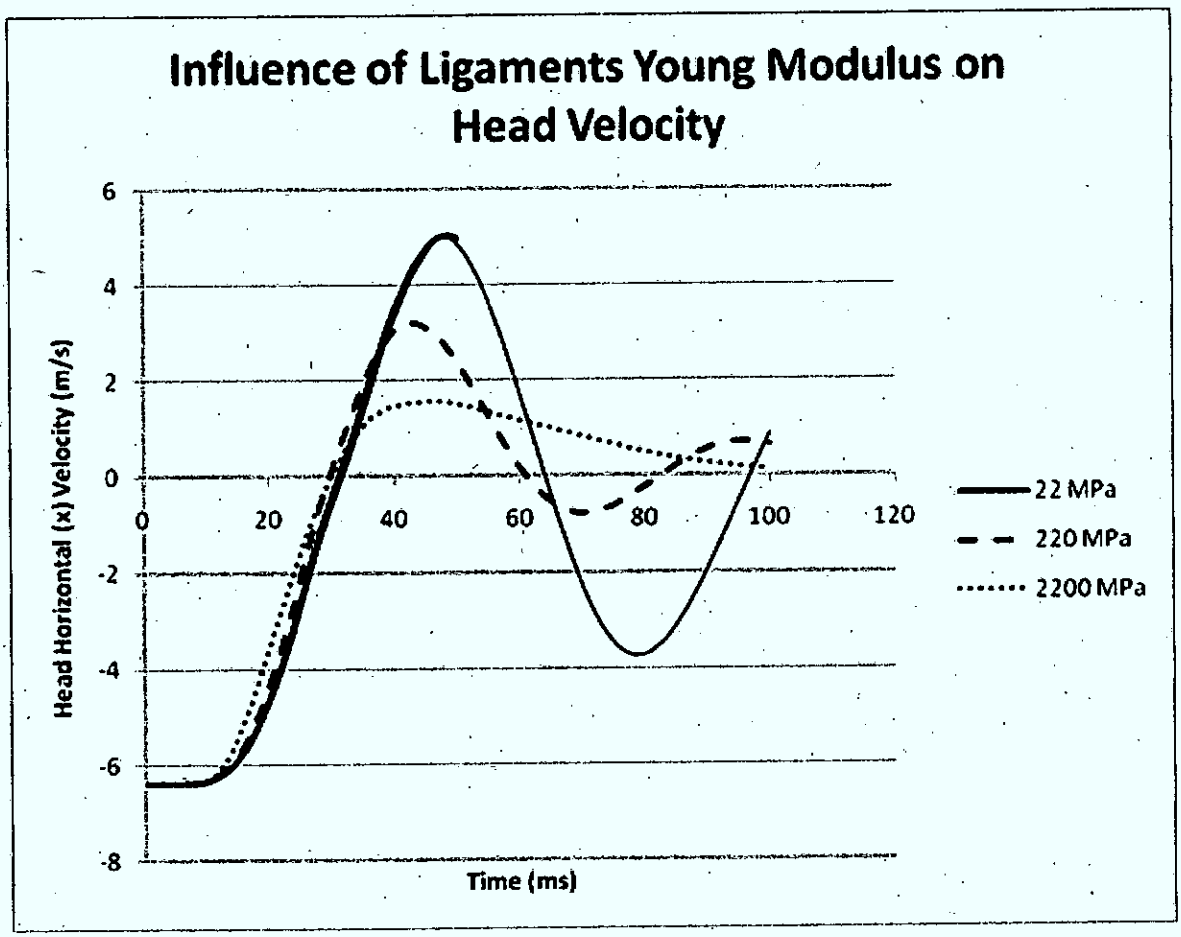
Influence of Ligaments Young Modulus on Head Velocity
Head Horizontal (x) Velocity (m/s)
6
4
2
0
-2
-4
-6
-8
0
20
40
60
80
100
120
Time (ms)
22 MPa
220 MPa
2200 MPa

FIGURE 5

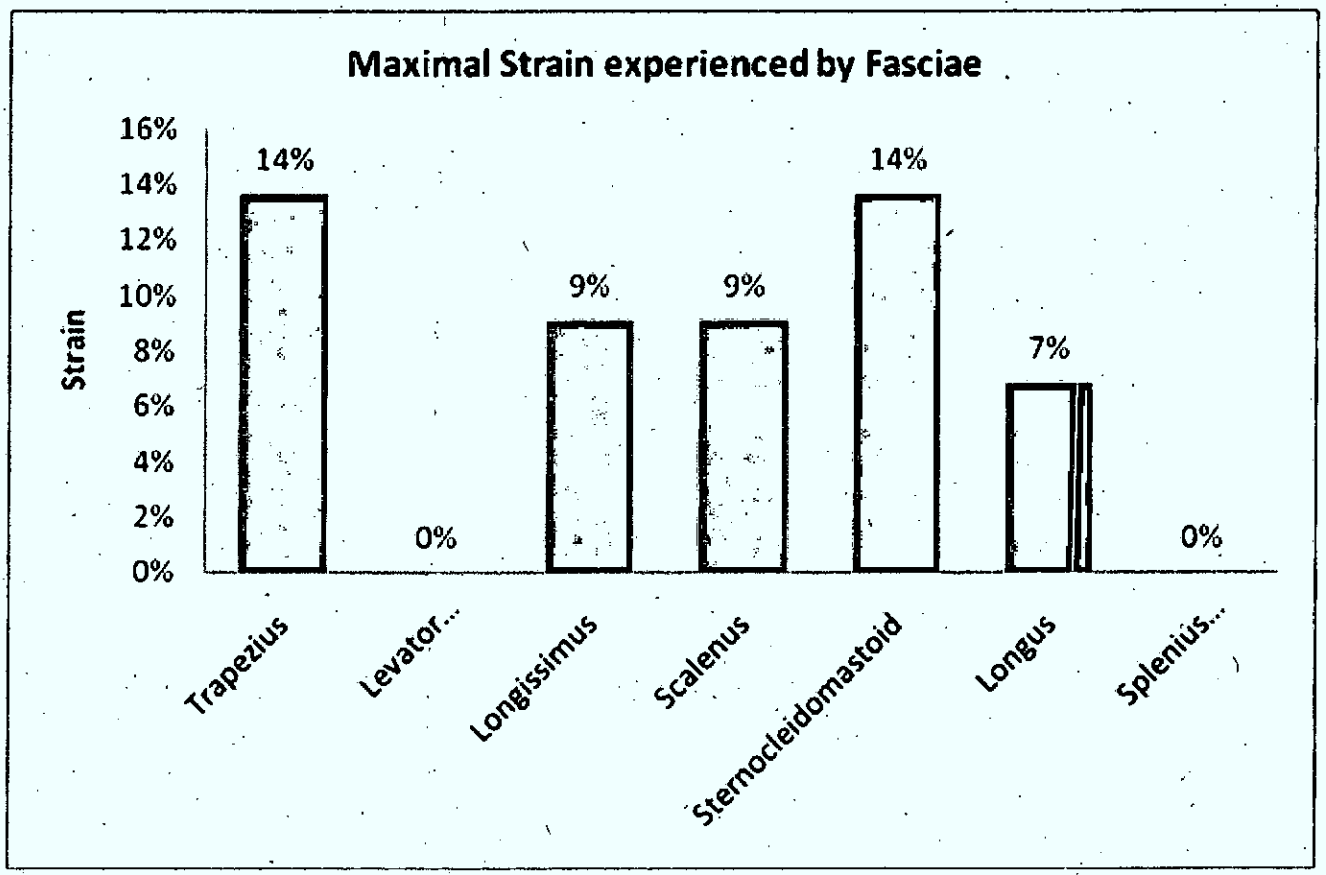
Maximal Strain experienced by Fasciae
Strain
16%
14%
12%
10%
8%
6%
4%
2%
0%
14%
0%
9%
9%
14%
7%
0%
Trapezius
Levator...
Longissimus
Scalenus
Sternocleidomastoid
Longus
Spleniús...

FIGURE 6

Vertebra	A (mm)	B (mm)	C (mm)	D (mm)
C1	-	-	47.6	-
C2	-	-	14.2	20.9
C3	13.5	16.9	14.2	18.8
C4	12.6	17.8	14.8	19.3
C5	12.2	19.0	15.2	22.4
C6	12.0	20.9	15.6	27.7
C7	13.0	24.6	15.5	34.9

TABLE 1

Joint	Rigidity (Nm/deg)
C0-C1	0.02
C1-C2	0.06
C2-C3	10.22
C3-C4	11.92
C4-C5	12.33
C5-C6	13.37
C6-C7	14.11

TABLE 2

Muscles	CSA (mm^2)	Origins	Insertions
Trapezius	150	Occipital bone Nuchal Ligament C7-T12	Shoulder
Levator Scapulae	150	C1-C4	Scapula
Longissimus	130	Thoracic Vertebrae	Mastoid
Scalenus	180	C2-C6	1st rib
Sternocleidomastoid	380	Clavicle	Mastoid
Longus	120	Occipital bone	Thoracic Vertebrae
Splenius Capitis	300	C7-T6	Mastoid

TABLE 3